Gö-VIP-19: PD Dr. Susanne Wienbeck
Institut für Diagnostische und Interventionelle Radiologie

Originalpublikation: Contrast-enhanced cone-beam breast-CT (CBBCT): clinical performance compared to mammography and MRI**. Eur Radiol.;** 2018 Sep; 28(9): 3731-3741.

Autoren: *Susanne Wienbeck[1], Uwe Fischer[2], Susanne Luftner-Nagel[2], Joachim Lotz[1], Johannes Uhlig[1]*

**Corresponding Author: Susanne Wienbeck*

[1] Institut für Diagnostische und Interventionelle Radiologie, Universitätsmedizin Göttingen, Robert-Koch-Str. 40, 37075 Göttingen

[2] Diagnostisches Brustzentrum Göttingen, Bahnhofsallee 1d, 37081 Göttingen

Zusammenfassung des wissenschaftlichen Inhalts

In der Brustkrebsfrüherkennung wird als primäres Untersuchungsverfahren nach wie vor die Mammographie eingesetzt, die allerdings insbesondere bei Frauen mit hoher Brustdichte deutliche Limitationen aufweist. Hiermit können bis zu 50% an Tumoren übersehen werden. Eine Verbesserung des Kontrastes zwischen Gewebe und Tumor bilden ihre technischen Weiterentwicklungen (DBT, CESM, Brust-CT und Brust-MRT), die einen Schwerpunkt in der radiologischen Forschung darstellen.

Eine speziell für die Untersuchung der weiblichen Brust entwickelte Computertomographie (Brust-CT), kann hierbei die Brustkrebsdiagnostik verbessern und die Anzahl unnötiger operativer und bioptischer Eingriffe reduzieren.

Durch unsere Arbeitsgruppe erfolgten erstmalig klinische prospektive Vergleichsstudien der kontrastmittelgestützten Brust-CT mit dem Brust-MRT, als etabliertes Verfahren im Rahmen der Abklärungsdiagnostik. Hierbei konnten wir demonstrieren, dass die kontrastmittelgestützte Brust-CT eine vergleichbare diagnostische Genauigkeit mit der Brust-MRT (77-83% vs. 88-89%) zur Malignitätsbeurteilung von Befunden in dichtem Brustgewebe (ACR Typ c/d) aufweist. Mittels Brust-CT ist es nicht nur möglich, maligne und benigne Brustläsionen zu unterscheiden: mittels quantitativer Analysen lassen sich auch Vorhersagen über den histopathologischen Subtyp und immunhistochemische Tumoreigenschaften treffen. Durch die Integration maschineller Lernverfahren in die Bewertung von Brust-CT Untersuchung, lässt sich in Zukunft möglicherweise die diagnostische Genauigkeit dieser Bildgebungsmodalität weiter steigern und insbesondere unerfahrene Untersucher in der Läsionsbeurteilung zu unterstützen.

Der Einsatz der Brust-CT in der klinischen Routine wird grundlegende Einfluss auf die Art und Weise haben, wie die Brustbildgebung in Zukunft durchgeführt wird und welchen Stellenwert sie neben den anderen bildgebenden Verfahren einnehmen wird.

Weitere Informationen:

PD Dr. Susanne Wienbeck
Universitätsmedizin Göttingen
Institut für Diagnostische und Interventionelle Radiologie
Robert-Koch-Str. 40, 37075 Göttingen
Telefon (Sekretariat): 0551/39-8965
E-Mail: susanne.wienbeck@med.uni-goettingen.de

European Radiology
https://doi.org/10.1007/s00330-018-5376-4

BREAST

Contrast-enhanced cone-beam breast-CT (CBBCT): clinical performance compared to mammography and MRI

Susanne Wienbeck[1] · Uwe Fischer[2] · Susanne Luftner-Nagel[2] · Joachim Lotz[1] · Johannes Uhlig[1]

Received: 17 August 2017 / Revised: 19 January 2018 / Accepted: 6 February 2018

Abstract

Objectives To evaluate the diagnostic accuracy of contrast-enhanced (CE) cone-beam breast computed tomography (CBBCT) in dense breast tissue and compare it to non-contrast (NC) CBBCT, mammography (MG) and magnetic resonance imaging (MRI).

Methods This prospective institutional review board-approved study included 41 women (52 breasts) with American College of Radiology (ACR) density types c or d and Breast Imaging Reporting and Data System (BI-RADS) 4 or 5 assessments in MG or ultrasound (US). Imaging modalities were independently evaluated by two blinded readers.

Results A total of 100 lesions (51 malignant, 6 high-risk, and 43 benign) were identified. For readers 1/2, respectively, and *p* values comparing CE-CBBCT to other modalities: diagnostic accuracy (AUC) for CE-CBBCT was 0.83/0.77, for MRI 0.88/0.89 (p = 0.2272/0.002), for NC-CBBCT 0.73/0.66 (p = 0.038/ 0.0186) and for MG 0.69/0.64 (p = 0.081/0.0207). CE-CBBCT sensitivity (0.88/0.78) was 37-39% higher in comparison to MG (0.49/0.41, $p < 0.001$ both) but inferior to MRI (0.98/0.96, p = 0.0253/0.0027). CE-CBBCT specificity (0.71/0.71) was numerically higher compared to MRI (0.61/0.69, p = 0.0956/0.7389).

Conclusions CBBCT diagnostic performance varied with the respective reader and experience. CE-CBBCT improved AUC and sensitivity in comparison to MG and NC-CBBCT, and was comparable to MRI in dense breast tissue. In tendency, specificity was higher for CE-CBBCT than MRI.

Key Points

- *CE-CBBCT diagnostic accuracy (AUC) was comparable to MRI in dense breasts.*
- *CE-CBBCT improved sensitivity and AUC in comparison to MG and NC-CBBCT.*
- *CE-CBBCT has inferior sensitivity but higher specificity than MRI.*
- *CE-CBBCT is a potential imaging alternative for patients with MRI contraindications.*

Keywords Breast · Cone-beam computed tomography · Contrast media · Mammography · Magnetic resonance imaging

Abbreviations

CBBCT	Cone-beam breast computed tomography
CE-CBBCT	Contrast-enhanced CBBCT
NC-CBBCT	Non-contrast CBBCT
MG	Mammography

Electronic supplementary material The online version of this article (https://doi.org/10.1007/s00330-018-5376-4) contains supplementary material, which is available to authorized users.

✉ Susanne Wienbeck
susanne.wienbeck@med.uni-goettingen.de

[1] Institute for Diagnostic and Interventional Radiology, University Medical Center Göttingen, Robert-Koch-Street 40, 37075 Göttingen, Germany

[2] Diagnostic Breast Center Göttingen, Bahnhofsallee 1d, Göttingen, Germany

Introduction

Mammography (MG) is the only breast imaging method affecting breast cancer mortality in quality-assured screening programs [1–3]. Nevertheless, a relevant limitation of MG is the reduced contrast between non-calcifying breast tumours and fat-free parenchyma, especially in dense breast tissue [4, 5]. Studies have shown a decrease of sensitivity and specificity in this population, with sensitivity reported as low as 30- 48% [4, 5]. Furthermore, breast density is an independent risk factor for breast cancer [4–6]. In this setting, additional imaging methods for improvement of diagnostic information and reduction of overlapping structures are warranted [7]. Advanced three-dimensional (3D) breast imaging modalities, including breast magnetic resonance imaging (MRI) and cone-beam breast computed tomography (CBBCT), may encounter the limitations of MG.

Published online: 28 March 2018

Contrast-enhanced MRI of the breast is the most sensitive technique for the detection of pre-invasive and invasive breast cancer [8, 9]. However, it may feature lower specificity, higher costs and lower availability than other imaging modalities [10–12]. In addition, the actual risk and long-term effects regarding gadolinium deposition are of growing concern [13, 14].

Dedicated CBBCT is a novel technique providing isotropic 3D images of the breast with high spatial resolution of up to 2.6 line pairs/mm and high contrast resolution that is able to detect a contrast difference of approximately 1% [15–17]. The additional application of intravenous contrast agents in CBBCT [contrast-enhanced CBBCT (CE-CBBCT)] has the potential to visualise tumour angiogenesis for acquisition of high spatial and contrast resolution as true three-dimensional (3D) data [18–20]. CE-CBBCT involves a breast CT scan prior to and after intravenous injection of iodinated contrast agent without breast compression. Previous studies have shown a superior cancer detection rate for CE-CBBCT over MG [15–17, 21]. However, to date there is no literature directly comparing the innovative contrast-enhanced breast imaging modality, CE-CBBCT, with the established breast MRI.

The purpose of this study was to evaluate the diagnostic accuracy of CE-CBBCT in dense breast tissue (type c and d) and compare it to MG, non-contrast (NC) CBBCT and MRI.

Materials and methods

This study was performed in accordance to the Declaration of Helsinki and received approval by the institutional review board (IRB). Written informed consent was obtained from all patients prior to inclusion. This prospective study was conducted from December 2015 to March 2017 at a university-affiliated reference breast-imaging center in central Germany.

The inclusion criteria for this prospective study were patients with ACR Breast Imaging Reporting and Data System (BI-RADS) category 4 or 5 lesions identified via MG or ultrasound (US), and dense or very dense breast tissue (type c or d) [22]. All study participants were examined via digital MG, NC-CBBCT, CE-CBBCT and breast MRI.

Exclusion criteria were male patients, history of allergic reaction to contrast agents, renal insufficiency, pregnancy and women aged less than 40 years (Fig. 1).

Image-guided breast biopsy was performed immediately after all imaging procedures if indicated. Reference standard in this study was histopathological verification via core-needle biopsy and/or surgery for suspected malignant lesions, or follow-up imaging after at least 12 months for probably benign lesions [23].

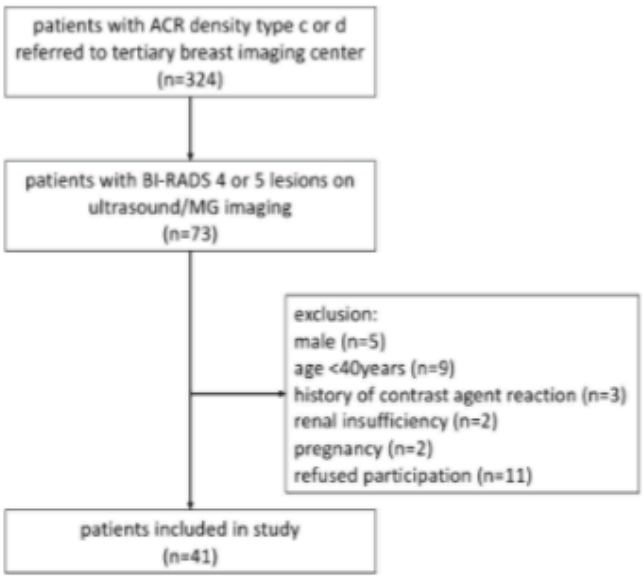

Fig. 1 Flow chart including the patient's enrolment and exclusion criteria

Imaging examinations

Digital mammography and ultrasound

Digital MG (Mammomat Inspiration, Siemens, Erlangen, Germany; Senographe Essential, GE Healthcare, Chicago IL, USA) and breast US (Logic S8 or E9 unit, 8-15 MHz frequency; GE Healthcare, Chicago, IL, USA) was performed in all patients. MG was obtained in two standard cranio-caudal and medio-lateral oblique views.

CBBCT examinations

CBBCT examinations (Koning Breast CT, CBCT 1000; Koning Corporation, West Henrietta, NY, USA) of the affected breast were performed at median 3 days after MG. CBBCT was conducted with a constant tube voltage of 49 kVp, and variable tube currents (between 50 and 200 mA) adjusted to the breast size and mammographic density [19, 24]. A complete contrast-enhanced breast CT scan comprised an initial non-contrast scan and post-contrast scan 2 min after injection of contrast media. For CE-CBBCT, a single-shot intravenous injection of 90 mL non-ionic contrast agent (iopromide, Ultravist 300; Bayer-Schering, Berlin, Germany) was performed at a rate of 3 mL/s using a power injector, followed by a 30-mL saline chaser. The CBBCT scanner utilised in our study only allowed for imaging of one breast at a time. To minimise contrast medium dose, bilateral CE-CBBCT examinations were performed by rapid repositioning of the second breast at a mean time of 3 min after primary contrast medium administration.

Post-acquisition image processing and reconstruction were performed to achieve isotropic reconstructed volumes using a soft tissue filter and a voxel size of 0.273 mm^3 (standard

mode). CE-CBBCT examination time, including patient positioning, was 8-10 min.

MRI examinations

MRI examinations were performed in median 4.5 days after CBBCT examination. The examinations were done on a 1.5-T whole-body scanner (Signa HDX, GE Healthcare, Chalfont St Giles, UK; Magnetom Sonata, Siemens Healthcare, Erlangen, Germany) via a dedicated open four-channel-breast surface coil in the prone position. The MRI examination included a fat-saturated T2-weighted inversion-recovery-sequence and dynamic T1-weighted FLASH 3D gradient echo sequences repetitively performed once before and 5 times after contrast injection (Gadovist®, Bayer HealthCare, Leverkusen, Germany). Examination time was 20-30 min for breast MRI.

CE-CBBCT and MRI examinations were performed independently of the menstrual cycle. The time interval between CE-CBBCT and MRI was greater than 24 h to prevent any contrast agent interaction in imaging and renal elimination.

Image analysis

Two breast radiologists with more than 7 years of breast imaging experience and also with 2 years of experience in dedicated CBBCT imaging independently evaluated all anonymised images. The image interpretation was done in three sessions. First, the two readers independently evaluated all MG images. A few days later, NC-CBBCT and CE-CBBCT studies were interpreted in random successive order on separate dates. After 2 weeks, the two readers read all MRI images independently. MG and CBBCT imaging studies in patients with bilateral breast lesions were randomly evaluated in separate sessions.

The readers were blinded to the patients' information and unaware of reference test results. Readers were aware of inclusion restriction to patients with BI-RADS 4 or 5 lesions on MG or US. The reading time was 10-15 min for NC- and CE-CBBCT images of one breast and 4-6 min for MRI exams. The reading time for CBBCT examination was in accordance with the results of Zhao et al. [17] with an average time of 12-17 min.

To compare the diagnostic accuracy of each imaging modality, the BI-RADS 5th edition [22] classification for both readers was correlated separately with histopathological diagnoses, adapted for NC-CBBCT and CE-CBBCT imaging from the MG and MRI part. All images were reviewed using the BI-RADS assessment scale as follows: BI-RADS 1, negative; BI-RADS 2, benign finding; BI-RADS 3, probably benign; BI-RADS 4, likely malignant; BI-RADS 5, malignant. A priori, papillomas were categorised as "benign" for analysis purposes [25, 26]. Breast lesions only detected on CBBCT and MRI but occult on mammograms were assigned an MG BI-RADS 1 score for analyses.

Statistical analysis

For descriptive statistics, continuous variables were expressed as median with interquartile range (IQR) and categorical variables as absolute number and percent. Kruskal-Wallis test was conducted to compare non-normally distributed breast lesion size, as indicated by Shapiro Wilks test ($p < 0.001$ for all imaging modalities).

The interobserver correlation coefficient (ICC) was used to assess the level of agreement on BI-RADS reading between the two readers [27]. In this study, an ICC less than 40% was considered as poor, 40-59% as fair, 60-74% as good and 75-100% as excellent.

For assessment of diagnostic test accuracy, test sensitivity, specificity and AUC [the area under the receiver-operating characteristic (ROC) curve] were calculated separately for each reader and imaging modality. Sensitivity was defined as the proportion of true-positive readings among true-positive and false-negative readings. Specificity was defined as the proportion of true-negative readings among true-negative and false-positive readings. For calculation of sensitivity and specificity, the BI-RADS score was dichotomised, labelling BI-RADS 1 and 2 as negative readings, and BI-RADS 3, 4 and 5 as positive readings. For calculation of the ROC curve and corresponding AUC in this diagnostic study setting, a modified four-point BI-RADS score was utilised as proposed by Jiang and Metz [28]: BI-RADS scores of 1 or 2 were summarised as indicating no probability of malignancy; all BI-RADS 0 lesions were discarded.

AUC, sensitivity and specificity across the imaging modalities were compared by each reader separately. For comparison of dependent AUCs, the method proposed by De Long et al. [29] was used. McNemar's test was utilised to compare test sensitivity and specificity.

Separate sensitivity analyses were conducted by inclusion of only histopathologically confirmed breast lesions.

All p values reported are two-sided. An alpha-level of 0.05 was considered statistically significant.

Results

Baseline patient characteristics

Of 49 eligible patients, 41 fulfilled the inclusion criteria and confirmed to participate. Of these, 30 (73.2%) were eventually diagnosed with histopathologically confirmed breast cancer. No patient withdrew consent or was lost to follow-up. Mild

contrast-agent-related adverse events with nausea on iodinated contrast agents were reported in two patients.

Median patient age at inclusion was 57.9 years (IQR, 48.9-64.9; range, 41.6-78.6 years). Fifteen patients (36.6%) were pre-menopausal at the time of imaging, 26 (63.4%) were post-menopausal. Fourteen patients (28.6%) presented with clinically palpable breast lesions. Breast density was categorised as "type c" in 26 patients (63.4%) and as "type d" in 15 patients (36.6%).

Breast lesions

One-hundred breast lesions were identified in the included patients. Thirty-six breast lesions were occult in MG and only detected by US. Forty-one breast lesions were occult in MG and detected by CBBCT and MRI. The median number of lesions per patient was 2 (IQR, 1-3; range, 1-8 lesions). In 19 patients, the left breast was affected (26.3%) and in 11 patients the right breast (26.8%). Another 11 patients (26.8%) had bilateral breast involvement. A total of 52 breasts were included. On CE-CBBCT, the majority of lesions had irregular (n = 49) or oval/round shape (n = 39) with indistinct (n = 47) or circumscribed margin (n = 30).

Median breast lesion size was 12.6 mm (IQR, 9.85-19.82 mm) on MG, 12.5 mm (IQR, 9.6-18.68 mm) on NC-CBBCT, 12.5 mm (IQR, 9.35-17.65 mm) on CE-CBBCT and 11.6 mm (IQR, 8.8-17.98 mm) on MRI. Kruskal-Wallis test revealed p = 0.7769 for differences in lesion size by imaging modalities.

The patients included 51 malignant breast lesions, 6 high-risk papillomas and 6 patients with benign lesions, as confirmed by biopsy or surgery. Another 37 benign breast lesions were confirmed after clinical follow-up more than 12 months later. Breast lesion subtypes and imaging appearance are detailed in Tables 1 and 2.

Diagnostic accuracy of imaging modalities

The AUCs of MG, NC-CBBCT, CE-CBBCT and MRI for reader 1 were 0.69, 0.73, 0.83 and 0.88, and for reader 2, 0.64, 0.66, 0.77 and 0.89, respectively. AUC differences were statistically significant between MG/CE-CBBCT and between NC-CBBCT/CE-CBBCT for both readers (p = 0.0081 and p = 0.038 for reader 1; p = 0.0207 and p = 0.0186 for reader 2). Significant differences for AUC between MRI and CE-CBBCT were only seen for reader 2 (p = 0.002).

Sensitivities of MG, NC-CBBCT, CE-CBBCT and MRI for reader 1 were 0.49, 0.57, 0.88 and 0.98, and for reader 2, 0.41, 0.47, 0.78 and 0.96, respectively. Differences in sensitivity were statistically significant between MG/CE-CBBCT and NC-CBBCT/CE-CBBCT for both readers (p < 0.001; p =

Table 1 Breast lesion subtypes

	%[a]
Benign	
Ductectasia	6
Fatty necrosis and cicatrix	2
Fibrosis	5
Fibroadenoma	5
Fibrocystic mastopathy	20
Intramammary lymph node	2
Mammary cyst	2
Mastitis	1
High-risk	
Papilloma	6
Malignant	
Ductal carcinoma in situ	3
Invasive ductal carcinoma	41
Invasive lobular carcinoma	3
Papillary mucinous carcinoma	1
lymphangiosis carcinomatosa	2
Intramammary metastasis	1

[a] Percent of each breast lesion subtype

Table 2 Breast lesions appearance by different imaging modalities

Imaging modality	Appearance	%[a]
MG	mass	73
	mass with microcalcification	6
	microcalcification (± asymmetry or architectural distortion)	15
	asymmetry	3
	others	3
NC-CBBCT	mass	73
	mass with microcalcification	8
	microcalcification (± asymmetry or architectural distortion)	15
	asymmetry	2
	others	2
CE-CBBCT	mass	71
	mass with microcalcification	11
	microcalcification (± asymmetry or architectural distortion)	12
	asymmetry	1
	others	5
MRI	mass	83
	NME	7
	mass and NME	3
	others	7

MG mammography, *NC* non-contrast, *CE* contrast-enhanced, *CBBCT* cone-beam breast-CT, *NME* non-mass enhancement, *MRI* magnetic resonance imaging

[a] Percent as detected by each imaging modality

Table 3 Summary of performance characteristics of mammography (MG), NC-CBBCT, CE-CBBCT and MRI for all patients (n = 100 lesions)

Reader	Method	AUC	p value[a]	Sensitivity	p value[a]	TP/TP + FN	Specificity	p value[a]	TN/TN + FP
1	MG	0.69 (0.61-0.77)	0.0081	0.49 (0.35-0.63)	<0.001	25/51	0.88 (0.78-0.97)	0.0455	43/49
2	MG	0.64 (0.55-0.72)	0.0207	0.41 (0.28-0.55)	<0.001	21/51	0.82 (0.71-0.93)	0.2253	40/49
1	NC-CBBCT	0.73 (0.65-0.81)	0.0380	0.57 (0.43-0.71)	0.0002	29/51	0.88 (0.78-0.97)	0.0325	43/49
2	NC-CBBCT	0.66 (0.58-0.75)	0.0186	0.47 (0.33-0.61)	<0.001	24/51	0.84 (0.73-0.94)	0.0578	41/49
1	CE-CBBCT	0.83 (0.76-0.9)	Reference	0.88 (0.79-0.97)	Reference	45/51	0.71 (0.59-0.84)	Reference	35/49
2	CE-CBBCT	0.77 (0.68-0.85)	Reference	0.78 (0.67-0.9)	Reference	40/51	0.71 (0.59-0.84)	Reference	35/49
1	MRI	0.88 (0.82-0.93)	0.2272	0.98 (0.94-1)	0.0253	50/51	0.61 (0.47-0.75)	0.0956	30/49
2	MRI	0.89 (0.84-0.95)	0.0020	0.96 (0.91-1)	0.0027	49/51	0.69 (0.56-0.82)	0.7389	34/49

All contrast-based methods showed higher AUCs and sensitivities in comparison to the other methods (MG and NC-CBBCT). CE-CBBCT and MRI were inferior to the both other modalities when comparing specificity

MG mammography, *NC* non-contrast, *CE* contrast-enhanced, *CBBCT* cone-beam breast-CT, *MRI* magnetic resonance imaging, *AUC* area under the receiver-operating curve, *TP* true positive, *FN* false negative, *TN* true negative, *FP* false positive

[a] All p values shown compared to CE-CBBCT by each reader separately

0.002). In comparison to CE-CBBCT, sensitivity of MRI was significantly higher for both readers (p = 0.0253; p = 0.0027).

Specificities of MG, NC-CBBCT, CE-CBBCT and MRI for reader 1 were 0.88, 0.88, 0.71 and 0.61, and for reader 2, 0.82, 0.84, 0.71 and 0.69, respectively. Specificity for CE-CBBCT was significantly lower than MG and NC-CBBCT only for reader 1 (p = 0.0455, p = 0.0325), while specificity differences between CE-CBBCT and MRI closely did not reach significance (p = 0.0956).

Diagnostic test accuracy results by each imaging modality are summarised in Table 3. Figures 2 and 3 aid in visual interpretation of the imaging modality accuracy and reader performance. Case reports demonstrating all imaging modalities in type c and type d density breasts are shown in Figs. 4 and 5.

Sensitivity analysis

Separate statistical analyses were conducted including only histopathologically approved breast lesions (n = 63). Results were comparable to the full cohort (n = 100) with highest AUC and sensitivity seen for MRI and CE-CBBCT, while specificity was largest for MG and NC-CBBCT. Comprehensive results are provided in the supplemental material.

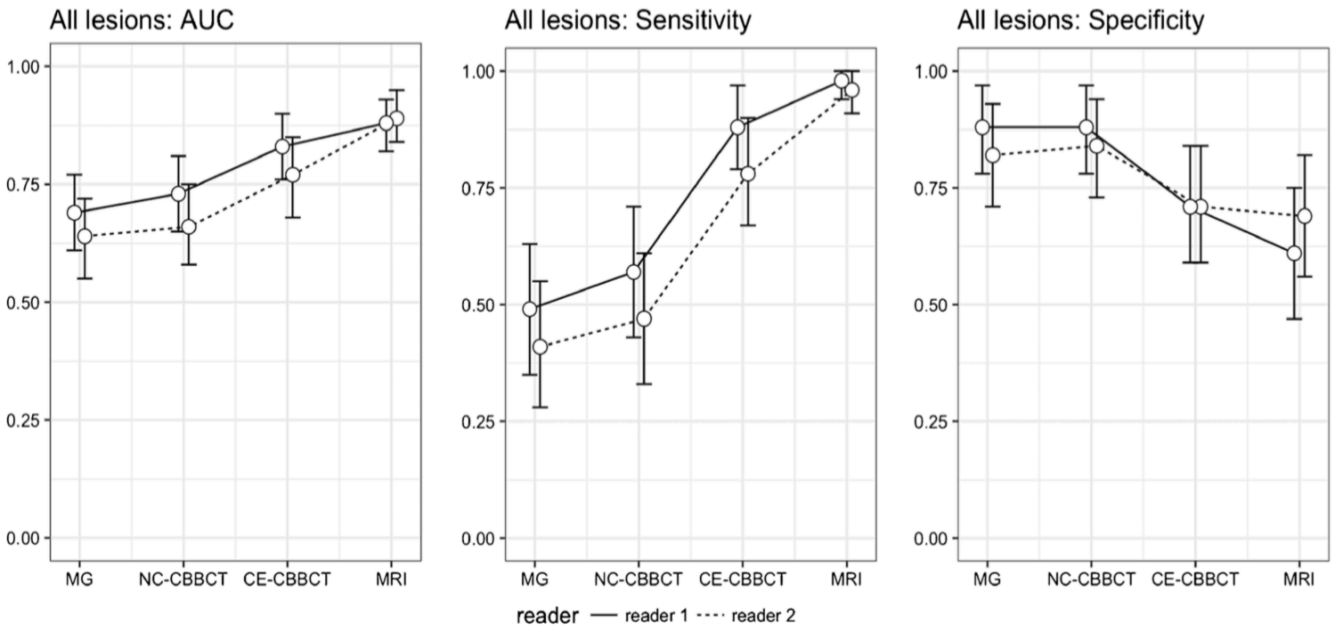

Fig. 2 Diagnostic accuracy for all lesion types in the study collective (n = 100 lesions) differentiating AUC, sensitivity and specificity with the different imaging modalities (MG, NC-CBBCT, CE-CBBCT and MRI). *MG* mammography, *NC* non-contrast, *CE* contrast-enhanced, *CBBCT* cone-beam breast-CT, *MRI* magnetic resonance imaging, *CI* confidence interval, *AUC* area under the receiver operating curve, *TP* true positive, *FN* false negative, *TN* true negative, *FP* false positive

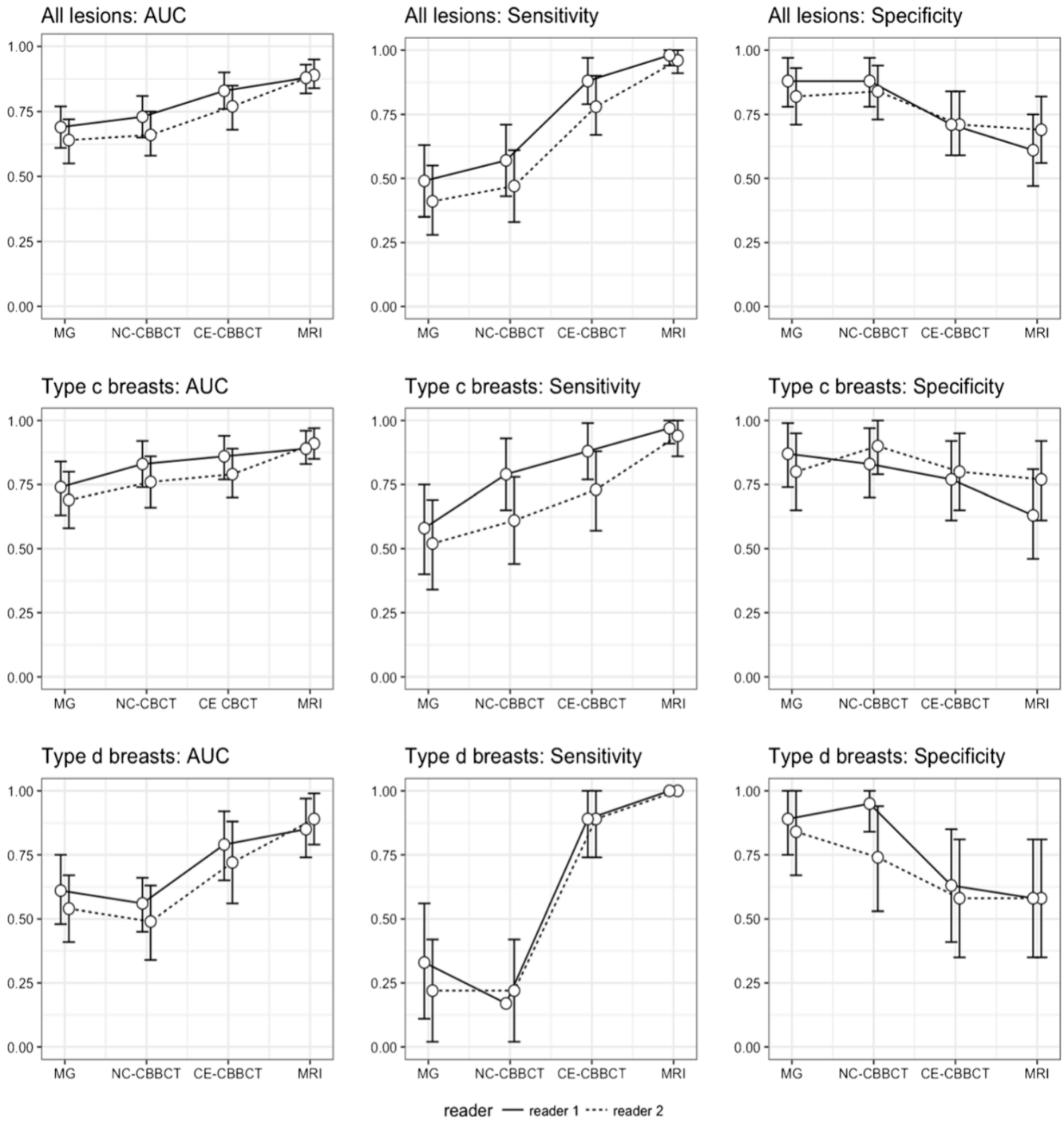

Fig. 3 Diagnostic accuracy for the overall study collective (n = 100 lesions) and for the density type c (n = 63 lesions) and d (37 lesions) group differentiating AUC, sensitivity and specificity with the different imaging modalities (MG, NC-CBBCT, CE-CBBCT and MRI). *MG* mammography, *NC* non-contrast, *CE* contrast-enhanced, *CBBCT* cone-beam breast-CT, *MRI* magnetic resonance imaging, *CI* confidence interval, *AUC* area under the receiver operating curve, *TP* true positive, *FN* false negative, *TN* true negative, *FP* false positive

Subgroup analysis by breast density

In total, 63 breast lesions were detected in type c breasts and 37 lesions in type d breasts (Fig. 3). For both density types and both readers, AUC and sensitivity were highest for CE-CBBCT and MRI, while specificity was highest for MG and NC-CBBCT.

Tables 4 and 5 detail diagnostic accuracy for both readers in type c and type d breasts.

Inter-reader agreement

Inter-reader agreement on BI-RADS was comparable and good to excellent across the different imaging modalities. The ICC for MG was ICC = 0.79 (95% CI, 0.70-0.85; p < 0.001), for NC-CBBCT ICC = 0.74 (95% CI, 0.63-0.82; p < 0.001), for CE-CBBCT ICC = 0.74 (95% CI, 0.63-0.82; p < 0.001), and for MRI, ICC = 0.76 (95% CI, 0.66-0.83; p < 0.001).

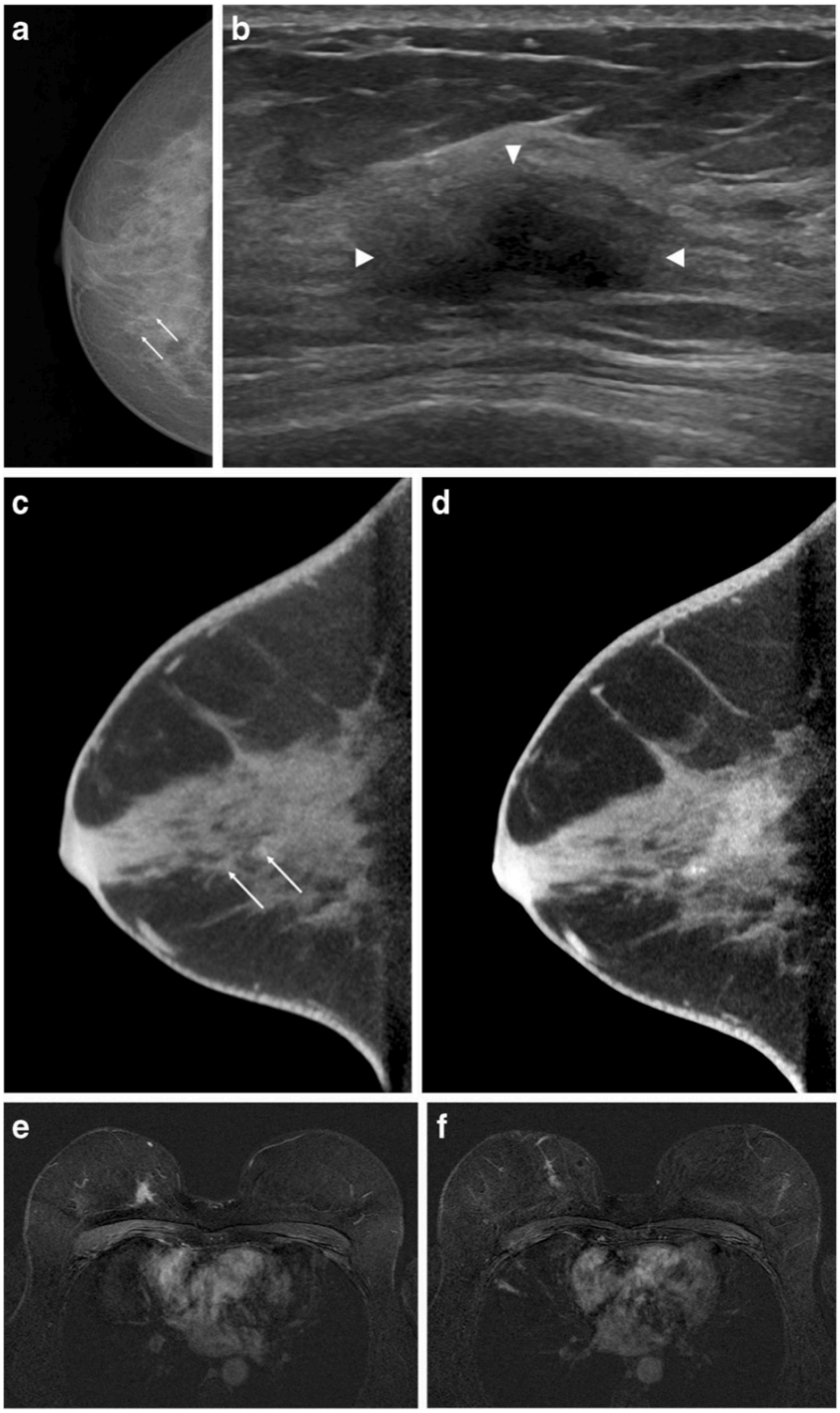

Fig. 4 A 51-year-old woman without clinical symptoms presented for routine mammography. **a** Diagnostic mammography in cranio-caudal view detected only a few microcalcifications, which were detected and judged as benign (*arrows*). The MG showed an ACR density type c of the breast. **b** In US, an associated hypoechoic mass with indistinct margins and with dorsal shadowing was seen (*arrowheads*). **c** With MG and corresponding NC-CBBCT the mass was not detected by both readers; only the microcalcifications were identified by one reader as malignant (*arrows*). **d** Corresponding CE-CBBCT and MRI showed an intensive enhancement of a mass (**e**) and an associated non-mass enhancing area (**f**), detected by both readers and was proved by surgery to be an invasive ductal carcinoma [(IDC) 24 mm] with ductal carcinoma in situ (DCIS), intermediate grade. The extent of this IDC with DCIS could only be correctly assessed by the contrast-based methods

Radiation dose

The median average glandular dose (AGD) by each breast for MG was 3.4 mGy (IQR, 2.76-4.34 mGy). For NC-CBBCT, the median AGD was 5.85 mGy (IQR, 5.85-7.5 mGy). A complete CE-CBBCT scan included the imaging of one breast before and 2 min after contrast media injection, resulting in a twofold increased total radiation dose compared to an NC-CBBCT scan (11.7 mGy; IQR, 11.7-14.98 mGy).

Discussion

To the best of our knowledge, our study is the first to compare the diagnostic accuracy of CE-CBBCT with NC-CBBCT, MG and MRI. Further, a robust design with two independent and blinded readers was implemented.

Our study demonstrated a higher overall AUC and sensitivity for contrast-based imaging modalities (CE-CBBCT and MRI) compared to MG and NC-CBBCT, while specificity was slightly lower. Therefore, CE-CBBCT could

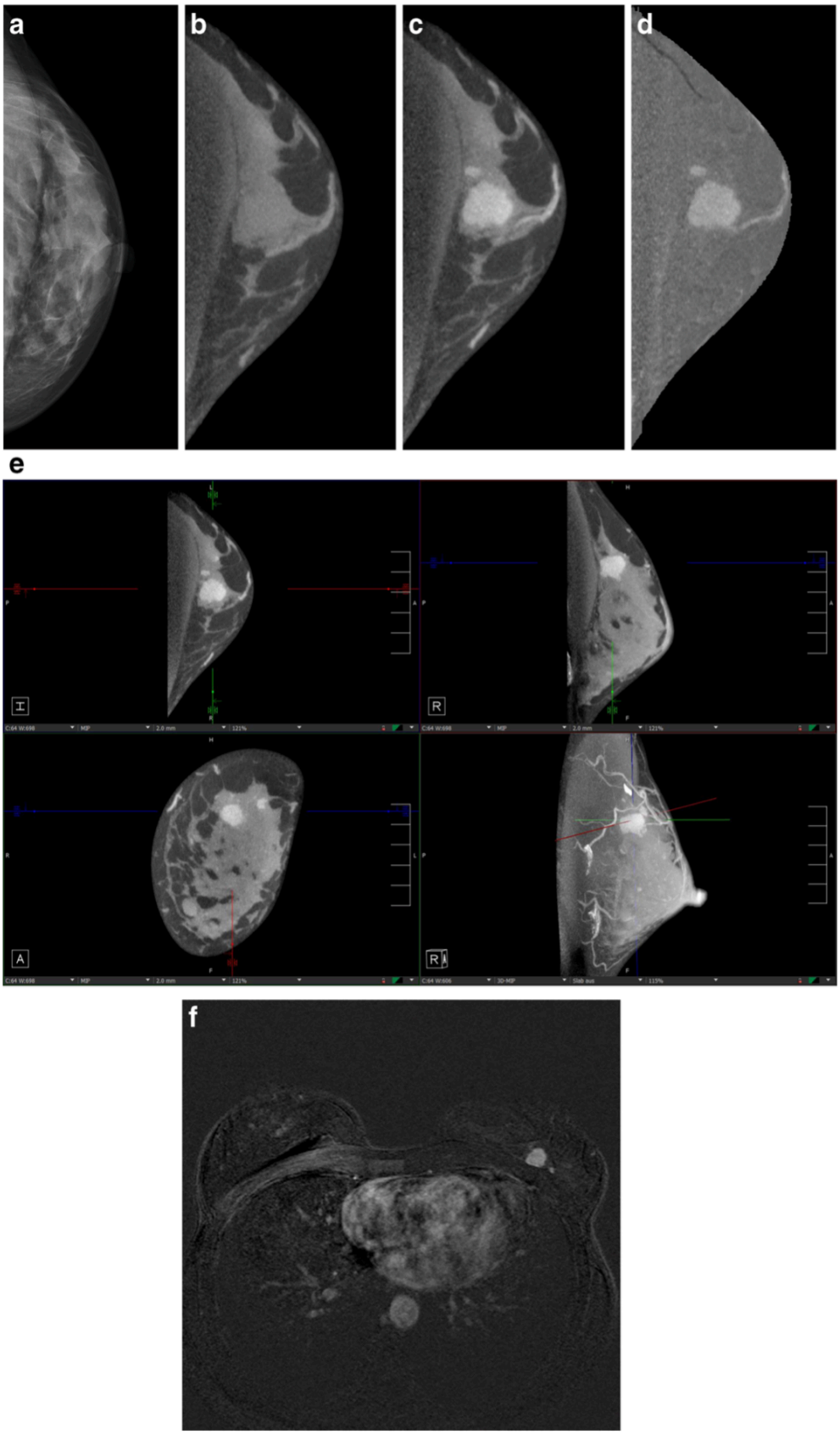

Fig. 5 A 47-year-old woman presenting with an IDC on the left breast (pT1c, 13 mm) and an IDC on the right side (pT1b, 7 mm), not shown. **a** The MG in cranio-caudal view showed an ACR density type d of the breast. **b** NC-CBBCT, **c** CE-CBBCT, **d** CBBCT subtracted images, **e** multiplanar projections of CE-CBBCT, 3D volume rendering illustrating the IDC (*cross*), **f** MRI. In MG and NC-CBBCT, both readers missed the IDC on the left side. Both readers correctly identified the IDC by CE-CBBCT and MRI. The smaller mass (5 mm) lateral of the IDC was reported false positive by both readers on CE-CBBCT and MRI. It was histopathologically proven to be fibrosis

serve as an imaging alternative for patients with MRI contraindications. Further CE-CBBCT benefits in comparison to breast MRI include a shortened examination time, as well as a more comfortable examination in patients with claustrophobia, and less noise. While both imaging modalities require contrast administration with potential side effects, the unknown long-term effects of gadolinium-based MRI contrast agents are of concern [13, 14].

Table 4 Summary of performance characteristics of mammography (MG), NC-CBBCT, CE-CBBCT and MRI for patients with breast density type c (n = 63 lesions)

Reader	Method	AUC	p value	Sensitivity	p value	TP/TP + FN	Specificity	p value	TN/TN + FP
1	MG	0.74 (0.63-0.84)	0.0312	0.58 (0.4-0.75)	0.0039	19/33	0.87 (0.74-0.99)	0.2568	26/30
2	MG	0.69 (0.58-0.8)	0.1026	0.52 (0.34-0.69)	0.0522	17/33	0.8 (0.65-0.95)	1.0000	24/30
1	NC-CBBCT	0.83 (0.74-0.92)	0.5092	0.79 (0.65-0.93)	0.1797	26/33	0.83 (0.7-0.97)	0.4142	25/30
2	NC-CBBCT	0.76 (0.66-0.86)	0.3783	0.61 (0.44-0.78)	0.0455	20/33	0.9 (0.79-1.01)	0.1797	27/30
1	CE-CBBCT	0.86 (0.77-0.94)	Reference	0.88 (0.77-0.99)	Reference	29/33	0.77 (0.61-0.92)	Reference	23/30
2	CE-CBBCT	0.79 (0.7-0.89)	Reference	0.73 (0.57-0.88)	Reference	24/33	0.8 (0.65-0.95)	Reference	24/30
1	MRI	0.89 (0.83-0.96)	0.4046	0.97 (0.91-1)	0.0833	32/33	0.63 (0.46-0.81)	0.1025	19/30
2	MRI	0.91 (0.85-0.97)	0.0063	0.94 (0.86-1)	0.0082	31/33	0.77 (0.61-0.92)	0.5637	23/30

For both readers, AUC and sensitivity were highest for CE-CBBCT and MRI, and specificity was comparable between the different imaging modalities

MG mammography, *NC* non-contrast, *CE* contrast-enhanced, *CBBCT* cone-beam breast-CT, *MRI* magnetic resonance imaging, *AUC* area under the receiver-operating curve, *TP* true positive, *FN* false negative, *TN* true negative, *FP* false positive

In terms of AUC and additional radiation exposure, women with density type d breasts tended to benefit more from CE-CBBCT versus NC-CBBCT and MG than those with density type c breasts.

CBBCT as a true 3D high-resolution technique reduces breast tissue overlap and has been shown to improve lesion conspicuity [19, 20, 30]. This mechanism could explain the higher diagnostic accuracy of NC-CBBCT in comparison to MG shown in different study settings [15–17, 19, 20, 30]. Our results are comparable to previous studies, although they applied a non-blinded study concept and did not focus on high-density breasts. Only He et al. [15] compared CBBCT with MG in women with high-density breasts and reported that NC-CBBCT improved both sensitivity and specificity.

When comparing CE-CBBCT to NC-CBBCT, improved diagnostic performance was attributed to contrast-enhanced detection of lesions that remained undetected with non-enhanced techniques.

Recent studies on CE-CBBCT demonstrated an increase in AUC and sensitivity compared to MG [15, 16, 31]. In concordance with earlier results, CE-CBBCT improved the detection of breast cancers in our study about 37-39% in comparison to digital MG. In a small study cohort, Seifert et al. [16] reported a high sensitivity for CE-CBBCT in comparison to NC-CBBCT and MG. Prionas et al. [21] found in a study on 46 women that malignant lesions showed better visualisation with CE-CBBCT than with NC-CBBCT and MG. In dense breast tissue, He et al. [15] showed highest AUC for CE-CBBCT compared to NC-CBBCT and MG in a consensus reading setting.

While in our study AUC and sensitivity were improved, CE-CBBCT specificity was up to 17% lower than for NC-CBBCT and MG. Nevertheless, CE-CBBCT showed slightly better specificity (2-10%) than MRI. Results by He et al. on improved specificity of CE-CBBCT (0.85) compared to NC-CBBCT (0.80) and MG (0.70) in patients with breast density types c and d could not be confirmed

Table 5 Summary of performance characteristics of mammography (MG), NC-CBBCT, CE-CBBCT and MRI for patients with breast density type d (n= 37 lesions)

Reader	Method	AUC	p value	Sensitivity	p value	TP/TP + FN	Specificity	p value	TN/TN + FP
1	MG	0.61 (0.48-0.75)	0.0919	0.33 (0.11-0.56)	0.0039	6/18	0.89 (0.75-1.04)	0.0956	17/19
2	MG	0.54 (0.41-0.67)	0.0627	0.22 (0.02-0.42)	0.0005	4/18	0.84 (0.67-1.01)	0.0956	16/19
1	NC-CBBCT	0.56 (0.45-0.66)	0.0073	0.17 (0-0.34)	0.0003	3/18	0.95 (0.84-1.05)	0.0339	18/19
2	NC-CBBCT	0.49 (0.34-0.63)	0.0108	0.22 (0.02-0.42)	0.0005	4/18	0.74 (0.53-0.94)	0.1797	14/19
1	CE-CBBCT	0.79 (0.65-0.92)	Reference	0.89 (0.74-1)	Reference	16/18	0.63 (0.41-0.85)	Reference	12/19
2	CE-CBBCT	0.72 (0.56-0.88)	Reference	0.89 (0.74-1)	Reference	16/18	0.58 (0.35-0.81)	Reference	11/19
1	MRI	0.85 (0.74-0.97)	0.3651	1 (1-1)	0.1573	18/18	0.58 (0.35-0.81)	0.5637	11/19
2	MRI	0.89 (0.79-0.99)	0.0615	1 (1-1)	0.1573	18/18	0.58 (0.35-0.81)	1.0000	11/19

For both readers, AUC and sensitivity was highest for CE-CBBCT and MRI, while specificity was highest for MG and NC-CBBCT

MG mammography, *NC* non-contrast, *CE* contrast-enhanced, *CBBCT* cone-beam breast-CT, *MRI* magnetic resonance imaging, *AUC* area under the receiver-operating curve, *TP* true positive, *FN* false negative, *TN* true negative, *FP* false positive

[15]. These discrepancies could be attributed to a non-independent reader setting in earlier studies, as well as to differences in patient populations [15, 16]. He et al. reported on younger patients, with 73% less than 50 years of age, while the mean age in our study was 57.9 years.

CE-CBBCT showed a higher specificity in type c breasts (reader 1/2: 0.77/0.8) in comparison to type d breasts (0.63/0.58). However, due to the small sample size of type d breasts (n = 37 lesions), all imaging modalities showed extreme and instable estimates for diagnostic accuracy, and the generalisability of this subgroup's findings is questionable.

Our study had several strengths. Only patients with imaging contraindications were excluded from the study. Moreover, all four imaging modalities were consistently performed in all patients, thus allowing direct comparisons of diagnostic performance. Finally, the two independent readers were blinded to histopathological results and the results of the other reader.

A major limitation is the large number of cases evaluated with imaging follow-up and missing histopathological assessment: even at a follow-up of 12 months, slow-growing breast malignancies cannot be fully excluded. However, since CBBCT as an innovative imaging modality has only recently become available, longer follow-up periods are unattainable. Nevertheless, comparable results were seen for the group of all histological approved lesions (n = 63). Further, our study is limited by the selection of patients to receive CE-CBBCT scan due to suspicious findings (BI-RADS 4 and 5 lesions) on MG and/or US. This design was chosen to avoid radiation of healthy women with additional CBBCT in this experimental setting. Therefore, a generalisation of our findings to the screening-eligible population is questionable. To avoid repeated contrast administration for bilateral breast involvement, patients were repositioned, resulting in a delayed second CE-CBBCT scan (3 min versus 2 min). This delay might distort contrast enhancement of otherwise similar lesions and presents a limitation as opposed to MRI that allows for simultaneous bilateral breast assessment. Finally, the comparably small sample size yields wide confidence intervals, large p values and limits further subgroup analyses.

Conclusions

In conclusion, our study demonstrates that the diagnostic accuracy of CE-CBBCT and MRI is superior to MG and NC-CBBCT in patients with dense breast tissue (ACR types c and d). Compared to MRI, CE-CBBCT showed in tendency a greater specificity and lower sensitivity, while AUC was comparable in the diagnostic setting depending on the readers experience.

Therefore, CE-CBBCT presents an imaging alternative for patients with MRI contraindications or for those concerned of gadolinium depositions, although CE-CBBCT radiation exposure and iodinated contrast media carry certain risks. Moreover, CBBCT offers a faster and more comfortable examination than MRI.

Future advances of CE-CBBCT envision advancements of iterative reconstruction technology to reduce radiation exposure and the implementation of dual-energy technology to suspend pre-contrast scans.

Acknowledgements The authors gratefully acknowledge the team of the Diagnostic Breast Center Göttingen, Germany for their continuous and excellent support.
The study's results were presented at the 2017
RSNA meeting in November 2017 in Chicago, USA.

Compliance with ethical standards

Guarantor The scientific guarantor of this publication is Prof. Dr. Joachim Lotz.

Conflict of interest The authors of this manuscript declare no relationships with any companies, whose products or services may be related to the subject matter of the article.

Statistics and biometry One of the authors has significant statistical expertise.

Informed consent Written informed consent was obtained from all subjects (patients) in this study.

Ethical approval Institutional Review Board approval was obtained.

Methodology
- prospective
- diagnostic or prognostic study
- performed at one institution

References

1. Jochelson M (2012) Advanced imaging techniques for the detection of breast cancer. Am Soc Clin Oncol Educ Book. https://doi.org/10.14694/EdBook_AM.2012.32.65:65-69
2. Welch HG, Passow HJ (2014) Quantifying the benefits and harms of screening mammography. JAMA Intern Med 174:448–454
3. Bleyer A, Welch HG (2012) Effect of three decades of screening mammography on breast-cancer incidence. N Engl J Med 367:1998–2005
4. Mandelson MT, Oestreicher N, Porter PL et al (2000) Breast density as a predictor of mammographic detection: comparison of interval- and screen-detected cancers. J Natl Cancer Inst 92:1081–1087
5. Kolb TM, Lichy J, Newhouse JH (2002) Comparison of the performance of screening mammography, physical examination, and breast US and evaluation of factors that influence them: an analysis of 27,825 patient evaluations. Radiology 225:165–175

6. Melnikow J, Fenton JJ, Whitlock EP et al (2016) Supplemental screening for breast cancer in women with dense breasts: a systematic review for the U.S. Preventive Services Task Force. Ann Intern Med 164:268–278
7. Smith A (2003) Fundamentals of digital mammography: physics, technology and practical considerations. Radiol Manage 25(18-24): 26–31 quiz 32-14
8. Sardanelli F, Podo F, Santoro F et al (2011) Multicenter surveillance of women at high genetic breast cancer risk using mammography, ultrasonography, and contrast-enhanced magnetic resonance imaging (the high breast cancer risk Italian 1 study): final results. Invest Radiol 46:94–105
9. Riedl CC, Luft N, Bernhart C et al (2015) Triple-modality screening trial for familial breast cancer underlines the importance of magnetic resonance imaging and questions the role of mammography and ultrasound regardless of patient mutation status, age, and breast density. J Clin Oncol 33:1128–1135
10. Berg WA, Blume JD, Cormack JB et al (2008) Combined screening with ultrasound and mammography vs mammography alone in women at elevated risk of breast cancer. JAMA 299:2151–2163
11. Dromain C, Balleyguier C, Muller S et al (2006) Evaluation of tumor angiogenesis of breast carcinoma using contrast-enhanced digital mammography. AJR Am J Roentgenol 187:W528–W537
12. Jochelson MS, Dershaw DD, Sung JS et al (2013) Bilateral contrast-enhanced dual-energy digital mammography: feasibility and comparison with conventional digital mammography and MR imaging in women with known breast carcinoma. Radiology 266: 743–751
13. Kanda T, Nakai Y, Oba H, Toyoda K, Kitajima K, Furui S (2016) Gadolinium deposition in the brain. Magn Reson Imaging 34: 1346–1350
14. Kanda T, Oba H, Toyoda K, Kitajima K, Furui S (2016) Brain gadolinium deposition after administration of gadolinium-based contrast agents. Jpn J Radiol 34:3–9
15. He N, Wu YP, Kong Y et al (2016) The utility of breast cone-beam computed tomography, ultrasound, and digital mammography for detecting malignant breast tumors: A prospective study with 212 patients. Eur J Radiol 85:392–403
16. Seifert P, Conover D, Zhang Y et al (2014) Evaluation of malignant breast lesions in the diagnostic setting with cone beam breast computed tomography (Breast CT): feasibility study. Breast J 20:364–374
17. Zhao B, Zhang X, Cai W, Conover D, Ning R (2015) Cone beam breast CT with multiplanar and three dimensional visualization in differentiating breast masses compared with mammography. Eur J Radiol 84:48–53
18. Lindfors KK, Boone JM, Newell MS, D'Orsi CJ (2010) Dedicated breast computed tomography: the optimal cross-sectional imaging solution? Radiol Clin North Am 48:1043–1054
19. O'Connell A, Conover DL, Zhang Y et al (2010) Cone-beam CT for breast imaging: Radiation dose, breast coverage, and image quality. AJR Am J Roentgenol 195:496–509
20. O'Connell AM, Kawakyu-O'Connor D (2012) Dedicated cone-beam breast computed tomography and diagnostic mammography: comparison of radiation dose, patient comfort, and qualitative review of imaging findings in BI-RADS 4 and 5 lesions. J Clin Imaging Sci 2:7
21. Prionas ND, Lindfors KK, Ray S et al (2010) Contrast-enhanced dedicated breast CT: initial clinical experience. Radiology 256: 714–723
22. Spak DA, Plaxco JS, Santiago L, Dryden MJ, Dogan BE (2017) BI-RADS(R) fifth edition: A summary of changes. Diagn Interv Imaging 98:179–190
23. Wallis M, Tardivon A, Helbich T, Schreer I, European Society of Breast I (2007) Guidelines from the European Society of Breast Imaging for diagnostic interventional breast procedures. Eur Radiol 17:581–588
24. Wienbeck S, Lotz J, Fischer U (2016) Review of clinical studies and first clinical experiences with a commercially available cone-beam breast CT in Europe. Clin Imaging 42:50–59
25. Purushothaman HN, Lekanidi K, Shousha S, Wilson R (2016) Lesions of uncertain malignant potential in the breast (B3): what do we know? Clin Radiol 71:134–140
26. Hoffmann O, Stamatis GA, Bittner AK et al (2016) B3-lesions of the breast and cancer risk - an analysis of mammography screening patients. Mol Clin Oncol 4:705–708
27. Shrout PE, Fleiss JL (1979) Intraclass correlations: uses in assessing rater reliability. Psychol Bull 86:420–428
28. Jiang Y, Metz CE (2010) BI-RADS data should not be used to estimate ROC curves. Radiology 256:29–31
29. DeLong ER, DeLong DM, Clarke-Pearson DL (1988) Comparing the areas under two or more correlated receiver operating characteristic curves: a nonparametric approach. Biometrics 44:837–845
30. Lindfors KK, Boone JM, Nelson TR, Yang K, Kwan AL, Miller DF (2008) Dedicated breast CT: initial clinical experience. Radiology 246:725–733
31. Aminololama-Shakeri S, Abbey CK, Gazi P et al (2016) Differentiation of ductal carcinoma in-situ from benign microcalcifications by dedicated breast computed tomography. Eur J Radiol 85:297–303